

# Multiple-baseline detection of a geostationary satellite with the Navy Precision Optical Interferometer

J. Thomas Armstrong<sup>a</sup>, Ellyn K. Baines<sup>a</sup>, Henrique R. Schmitt<sup>a</sup>, Sergio R. Restaino<sup>a</sup>, James H. Clark III<sup>a</sup>, James A. Benson<sup>b</sup>, Donald J. Hutter<sup>b</sup>, Robert T. Zavala<sup>b</sup>

<sup>a</sup>Remote Sensing Division, Naval Research Laboratory, Washington, DC 20375, USA;

<sup>b</sup>US Naval Observatory, Flagstaff Station, Flagstaff, AZ 86001, USA

## ABSTRACT

We describe multi-baseline observations of a geostationary satellite using the Navy Precision Optical Interferometer (NPOI) during the glint season of March 2015. We succeeded in detecting DirecTV-7S with an interferometer baseline length of 8.8 m on two nights, with a brief simultaneous detection at 9.8 m baseline length on the second night. These baseline lengths correspond to a resolution of  $\sim 4$  m at geostationary altitude. This is the first multiple-baseline interferometric detection of a satellite.

**Keywords:** geostationary satellites, optical interferometry, imaging, telescope arrays

## 1. INTRODUCTION

Developing the ability to resolve geostationary satellites (geosats) from the ground for Space Situational Awareness is currently drawing wide interest. The largest single telescopes are just capable of resolving the large-scale structure of these satellites,<sup>1</sup> but resolving details requires the use of other techniques, such as optical interferometry.

The Navy Precision Optical Interferometer (NPOI)<sup>2,3</sup> is the first, and so far only, interferometer to succeed in detecting a satellite. We observed DirecTV-9S with a 16 m baseline during the glint season of March 2008, with followup observations in 2009<sup>4</sup> resulting in a glint model consisting of a resolved ( $\gtrsim 3.7$  m) and an unresolved ( $\sim 1$  m) component, with roughly equal fluxes.

One of the lessons from those observations is that the baseline length  $B$  of 16 m, the shortest available at the NPOI at the time, is somewhat too long for observing these targets, for which the typical size scale is several meters. The  $\lambda = 556$  nm to 845 nm wavelength range used in those observations produced a resolution  $\theta_{\text{res}} \approx \lambda/B \approx 35$  nrad to 50 nrad, corresponding to 1.3 to 2 m at geostationary altitude. Structure at that scale produces a fringe contrast  $V \approx 0.2$ , and structure that is only 20% larger than  $\theta_{\text{res}}$  produces no fringe contrast at all. At still larger scales, the fringe contrast recovers, but only weakly.

The lack of shorter baselines puts us at a disadvantage in two ways. First, it makes it difficult or impossible to detect and track fringes in real time and thereby adjust the internal optical paths in the interferometer, particularly because atmospheric turbulence over the array elements forces us to detect fringes and readjust optical paths on 20 ms timescales. Second, if we have data only from long baselines, those data do a poor job of characterizing the larger-scale structure of the target. A better representation of the larger scales representative of the satellite bus requires data from shorter baselines, or in interferometric parlance, sampling smaller  $u - v$  spacings, where  $u$  and  $v$  are the spatial frequencies  $B_{\text{EW}}/\lambda$  and  $B_{\text{NS}}/\lambda$  sampled toward the target by the east-west and north-south components of the baseline.

Since 2009, the NPOI has brought several new array stations into operation that make shorter baselines available (see Fig. 1). In particular, we now have an 8.8 m baseline between stations W4 and AC, which yields resolutions of 2.3 to 3.5 m at geostationary altitude, and a 9.8 m baseline between stations AC and E3. Having two short baselines that share an array element, such as these, makes it possible to “bootstrap” them together to make a third baseline, W4 to E3, of 18.6 m. If fringes are detected and tracked on the two shorter baselines,

---

Further author information: (Send correspondence to J.T.A.) E-mail: tom.armstrong@nrl.navy.mil, Telephone: 1 202 767 0669

Report Documentation Page			Form Approved OMB No. 0704-0188		
Public reporting burden for the collection of information is estimated to average 1 hour per response, including the time for reviewing instructions, searching existing data sources, gathering and maintaining the data needed, and completing and reviewing the collection of information. Send comments regarding this burden estimate or any other aspect of this collection of information, including suggestions for reducing this burden, to Washington Headquarters Services, Directorate for Information Operations and Reports, 1215 Jefferson Davis Highway, Suite 1204, Arlington VA 22202-4302. Respondents should be aware that notwithstanding any other provision of law, no person shall be subject to a penalty for failing to comply with a collection of information if it does not display a currently valid OMB control number.					
1. REPORT DATE <b>2015</b>	2. REPORT TYPE		3. DATES COVERED <b>00-00-2015 to 00-00-2015</b>		
4. TITLE AND SUBTITLE <b>Multiple-baseline detection of a geostationary satellite with the Navy Precision Optical Interferometer</b>			5a. CONTRACT NUMBER		
			5b. GRANT NUMBER		
			5c. PROGRAM ELEMENT NUMBER		
6. AUTHOR(S)			5d. PROJECT NUMBER		
			5e. TASK NUMBER		
			5f. WORK UNIT NUMBER		
7. PERFORMING ORGANIZATION NAME(S) AND ADDRESS(ES) <b>Remote Sensing Division, Naval Research Laboratory,,Washington,,DC, 20375</b>			8. PERFORMING ORGANIZATION REPORT NUMBER		
9. SPONSORING/MONITORING AGENCY NAME(S) AND ADDRESS(ES)			10. SPONSOR/MONITOR'S ACRONYM(S)		
			11. SPONSOR/MONITOR'S REPORT NUMBER(S)		
12. DISTRIBUTION/AVAILABILITY STATEMENT <b>Approved for public release; distribution unlimited</b>					
13. SUPPLEMENTARY NOTES <b>Proc. of SPIE Vol. 9617 961709-1</b>					
14. ABSTRACT <b>We describe multi-baseline observations of a geostationary satellite using the Navy Precision Optical Interferometer (NPOI) during the glint season of March 2015. We succeeded in detecting DirecTV-7S with an interferometer baseline length of 8.8 m on two nights, with a brief simultaneous detection at 9.8 m baseline length on the second night. These baseline lengths correspond to a resolution of 4 m at geostationary altitude. This is the first multiple-baseline interferometric detection of a satellite.</b>					
15. SUBJECT TERMS					
16. SECURITY CLASSIFICATION OF:			17. LIMITATION OF ABSTRACT <b>Same as Report (SAR)</b>	18. NUMBER OF PAGES <b>9</b>	19a. NAME OF RESPONSIBLE PERSON
a REPORT <b>unclassified</b>	b ABSTRACT <b>unclassified</b>	c THIS PAGE <b>unclassified</b>			

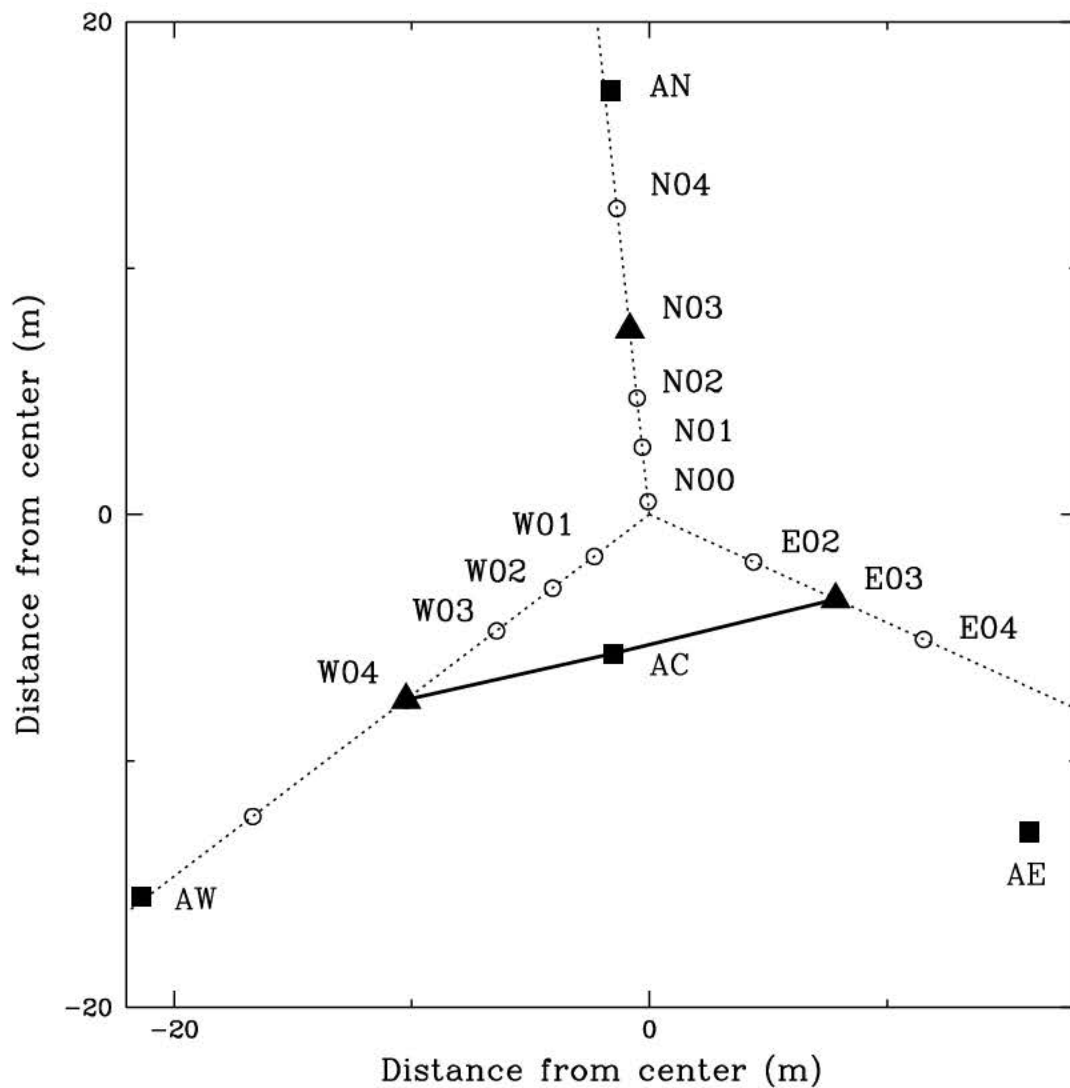


Figure 1. Layout of the inner stations of the NPOI. The black squares are the astrometric stations AW, AC, AE and AN. The black triangles show the new imaging stations, W04, E03 and N03, commissioned for the observation of geosat glints. The black lines show the baselines W04-AC and AC-E03 used in these observations of DirecTV-7S.

the third baseline is also correctly phased, and it can take data without fringes being detectable on it in real time, a concept due originally to Roddier.<sup>5</sup>

Using three or more array elements also allows us to obtain closure phases, the sum of the fringe phases around the triangle of baselines. Because atmospheric perturbations of the baseline phases cancel in the sum,<sup>6</sup> these closure phases represent some (though not all) of the phase information of the image of the target. In particular, they can be used to better determine the relative locations of the components of the satellite.

## 2. OBSERVATIONS

### 2.1 NPOI

The 12 cm apertures of the NPOI's array elements, in conjunction with atmospherically-induced fringe motion that requires adjusting the internal path lengths at  $\sim 50$  Hz, limit the NPOI's sensitivity to visual-band

magnitudes  $V \lesssim 6$  mag. During most of the year, most geosats are much fainter, typically  $V \sim 10$  mag to 15 mag. Twice yearly, however, some satellites whose solar-panel arrays are oriented north-south can glint brightly by specular reflection of sunlight. Because we see the Sun reflected by the panels, the “glint season” occurs when the apparent declination of the Sun is the same as that of the satellites. From the NPOI, the geosat belt is at an apparent declination of  $-6^\circ$ , so the glint seasons, which are about 10 days long, are centered on March 1 and October 11, when the Sun is south of the Equator. Glints can be as bright as 1<sup>st</sup> magnitude, and typically last for 5 to 20 min each night.

We observed DirecTV-7S with the NPOI on the nights of 2015 March 5 and 6, using stations W4, AC, E3, and N3. We used four, rather than the maximum of six, stations in part because having fewer baselines, and hence fewer interference fringes, in the data makes detecting the fringes easier. In the event, N3 had a malfunction, leaving us with three stations and three baselines. For most of the February 26 to March 6 observing run, the array configuration was purely academic due to heavy snowfall, and although the skies cleared for the 5<sup>th</sup> and 6<sup>th</sup>, we had very poor seeing (high atmospheric turbulence).

The NPOI “Classic” beam combiner<sup>3</sup> used for these observations uses pathlength modulation to scan the interference fringes. The feed beam from each array element traverses a delay line, which imposes a 500 HZ triangle wave modulation on each beam. Modulation amplitudes are multiples of 1  $\mu\text{m}$ , creating triangle-wave optical path difference (OPD) variations with amplitudes of 1, 2, or 3  $\mu\text{m}$  between beams when they are combined. We used two of the Classic combiner’s three output beams, each fed to a spectrograph that records 16 spectral channels in the 556–845 nm wavelength range. Spectrograph 1 recorded all three baselines simultaneously, while baseline W4-AC appeared as well in spectrograph 2. The Classic combiner collects data for an integral number of wavelengths in each wavelength channel, so for OPD amplitudes of 1, 2, and 3  $\mu\text{m}$ , the fringe frequencies in the data are  $k = 1, 2$ , and 3 fringes per modulation period, corresponding to baselines W4-E3, W4-AC and AC-E3, respectively.

## 2.2 Supporting observations

Observing geosats with an interferometer differs from observing stars in two ways: we don’t know precisely where they are, and we don’t have much time to find them. As for the position, pointing the individual array elements at the geosat is straightforward; what is difficult is knowing the OPD for the particular target. For a 9 m baseline, shifting the OPD by 100  $\mu\text{m}$  corresponds to shifting the sky position at which the baseline is pointed by 2.3 arcsec, while the position calculated from the satellite’s two-line orbital elements (TLEs) published on line is typically 10 times less precise. Since searching 100  $\mu\text{m}$  in OPD space can take several minutes, knowing the satellite position to 1 arcsec or better can make the difference between finding fringes at the correct OPD while the satellite is still glinting and missing the glint altogether.

We used the Naval Observatory Flagstaff Station 40-inch telescope in the R band ( $\lambda \approx 660$  nm) to measure the positions and drift rates of our targets until the glints became bright enough at  $R \approx 7$  to saturate the camera. We then extrapolated forward for the next hour to generate positions for steering the OPDs at the NPOI. The positional uncertainty from our position measurements and extrapolations was better than 1 arcsec.

## 3. RESULTS

### 3.1 Photometry

The 16 spectral channels of the NPOI provide a means of doing low-precision comparative photometry. The uncalibrated spectrum of DirecTV-7S is presented in Fig. 2, along with the spectrum of a G9 giant star,  $\zeta$  Hydrae, observed the same night. The spectrum of the star was divided by 1.9 in order to match the spectrum of DirecTV-7S at 845 nm and highlight the color difference between the star and the satellite. From the  $V$  ( $\lambda 550$  nm) and  $I$  ( $\lambda 805$  nm) magnitudes of  $\zeta$  Hydrae (3.10 mag and 1.90 mag, respectively<sup>7</sup>) and our measured flux ratios, we calculate that DirecTV-7S magnitudes were  $V = 4.5$  mag and  $I = 2.6$  mag during the period when fringes were detected. With  $V - I = 1.9$  mag, this satellite is significantly redder than the Sun ( $V - I = 0.70$  mag<sup>8</sup>), the source of light it reflects. This result is consistent with other observations of geostationary satellites.<sup>9–11</sup>

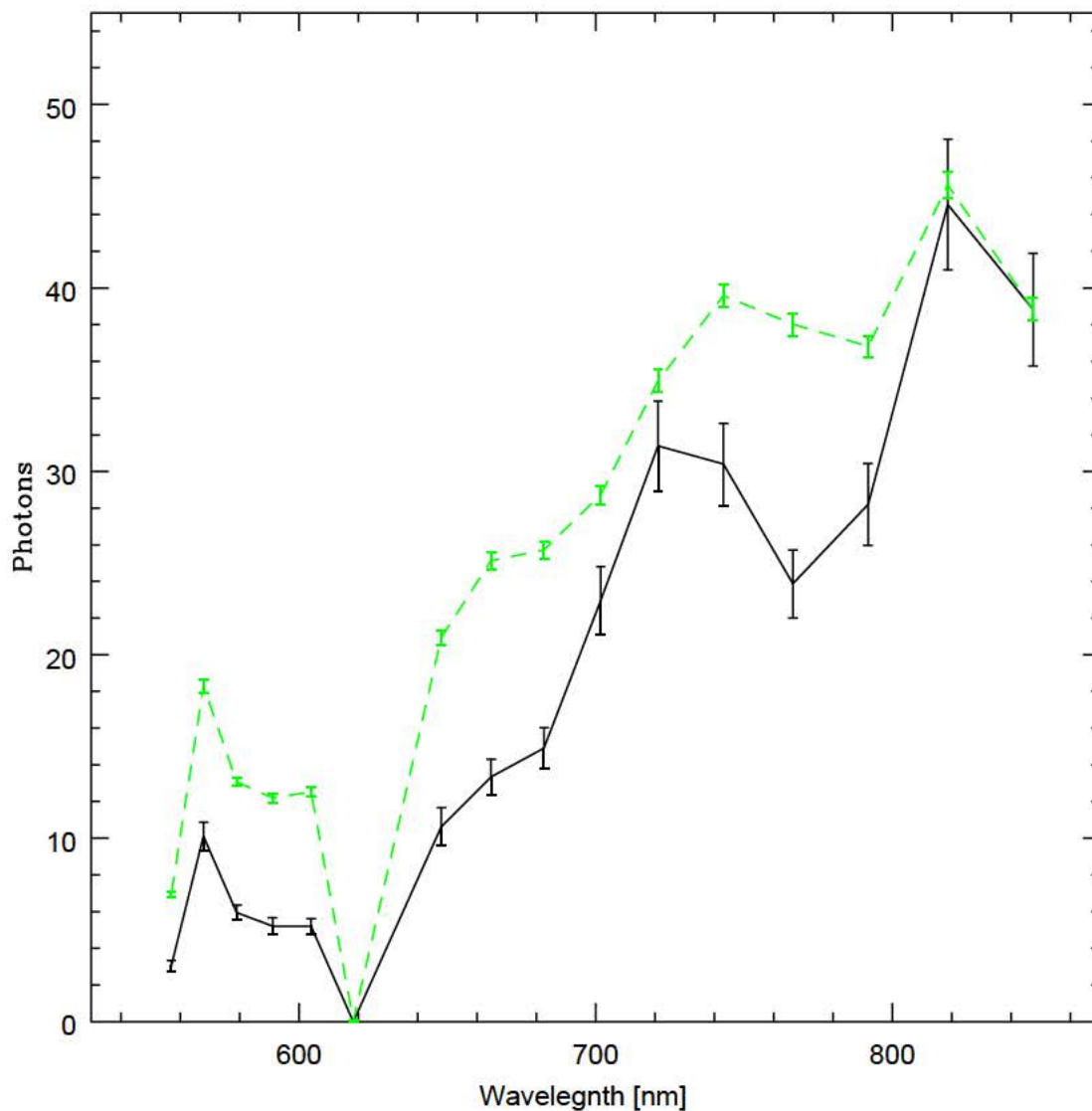


Figure 2. Uncalibrated spectrum of the geosat DirecTV7S observed with NPOI Classic spectrograph 1 (solid black line) and the star  $\zeta$  Hydrae (HR 3547; green dashed line). The vertical axis shows the number of photons detected per 2 ms frame. The 618 nm channel is dead and has been set to zero.

We obtained fringes on DirecTV-7S on a single baseline, W4-AC on the night of 2015 March 5 (UT), but because the combiner software was searching for a second baseline, the data were not recorded. The next night, fringe detection continued to be intermittent due to poor weather, but we were able to detect and record fringes over a period of 27 s, during which we tracked the fringe on baseline W4-AC for approximately 4 s and the fringe on baseline AC-E3 for a smaller fraction of the time. The observations were further complicated by the fact that they were done during the last days of the glinting season, which means that the glints were shorter in duration and less extreme in brightness than they would have been at the peak of the season.

The fringe power spectra shown in Figs. 3 and 4 show the detection from March 6 in each of 12 spectral channels. Figure 3 shows spectrograph 2, which observed only baseline W4-AC at a fringe scanning frequency  $k = 2$  cycles per modulation period. The bias-subtracted fringe power (green trace) shows a strong signal in the 845 nm channel (ch1), with declining fringe power as the wavelength gets shorter. Figure 4 shows spectrograph 1, with which observed all three baselines were observed. Again, there is a strong signal at  $k = 2$  from baseline W4-AC in channel 1, but there is also a weaker signal from baseline AC-E3 at  $k = 3$ . These fringe power signals can be followed to channel 7 (700 nm) or 8 (681 nm).

Figure 4 does not show evidence of a fringe at  $k = 1$ , corresponding to the bootstrapped W4-E3 baseline, due to some combination of the bad weather, the size of the target, and the short time over which we detected fringes, especially on the AC-E3 baseline.

#### 4. FUTURE WORK

We are currently analyzing our data from DirecTV-7S and from stars observed during 2015 March 6 to determine methods of eliminating frames taken during moments when the fringes were not present and of averaging the on-fringe data. With appropriately filtered data, we will be in a position to model the data and determine the sizes and relative fluxes of the glinting structures.

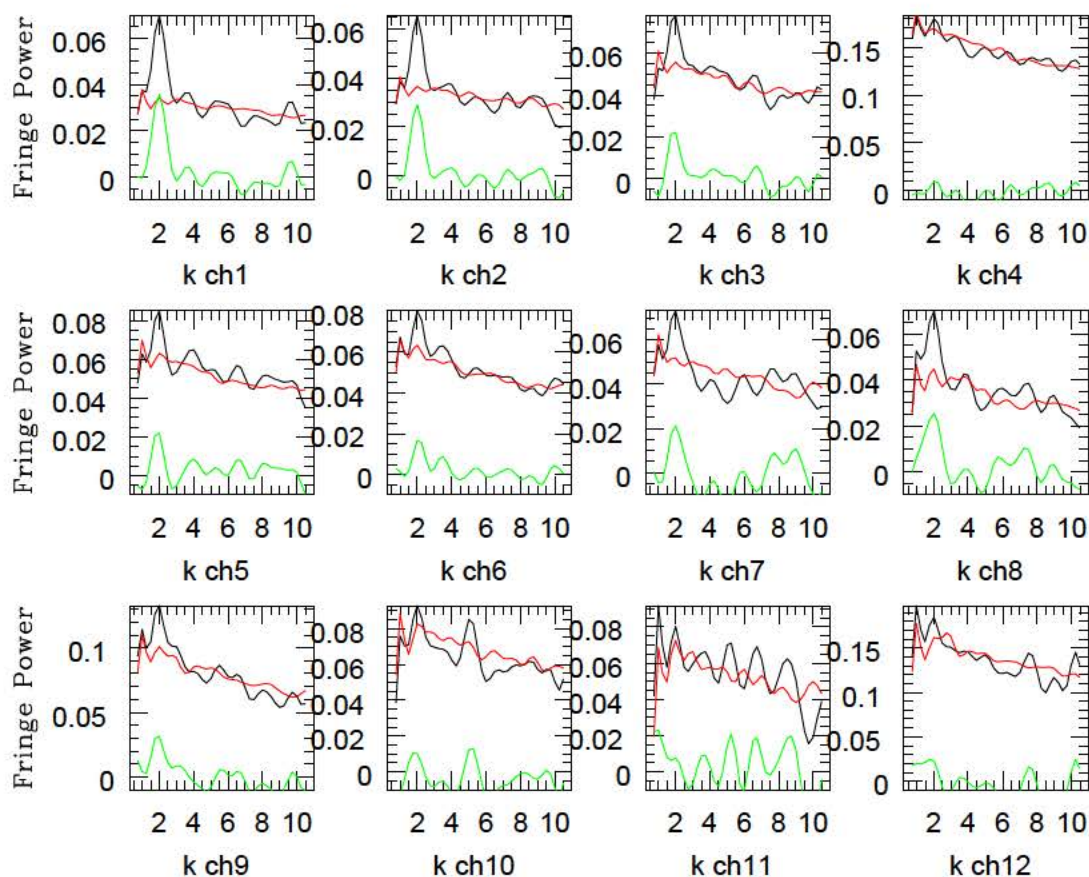
The next glint season at the NPOI occurs in early October 2015. We plan to use the same compact NPOI configuration. Backend software and hardware improvements now under way may allow us to record data in 32 spectral channels (845 nm to 450 nm) with all three of the output beams of the current Classic combiner.

#### ACKNOWLEDGMENTS

The NPOI is a joint project of the Naval Research Laboratory and the US Naval Observatory in cooperation with Lowell Observatory, and is funded by the Oceanographer of the Navy and by 6.1 base funding from the Office of Naval Research.

#### REFERENCES

- [1] Drummond, J. and Rast, R., "First Resolved Images of a Spacecraft in Geostationary Orbit with the Keck II 10 m Telescope," in [*Proceedings of the Advanced Maui Optical and Space Surveillance Technologies Conference*], Ryan, S., ed., E21–E26, The Maui Economic Development Board, Wailea (2010).
- [2] Armstrong, J. T., Mozurkewich, D., Rickard, L. J., Hutter, D. J., Benson, J. A., Bowers, P. F., Elias II, N. M., Hummel, C. A., Johnston, K. J., Buscher, D. F., Clark III, J. H., Ha, L., Ling, L.-C., White, N. M., and Simon, R. S., "The Navy Prototype Optical Interferometer," *Astrophys. J.* **496**, 550–571 (1998).
- [3] Armstrong, J. T., Hutter, D. J., Baines, E. K., Benson, J. A., Bevilacqua, R. M., Buschmann, T., Clark III, J. H., Ghasempour, A., Hall, J. C., Hindsley, R. B., Johnston, K. J., Jorgensen, A. M., Mozurkewich, D., Muterspaugh, M. W., Restaino, S. R., Shankland, P. D., Schmitt, H. R., Tycner, C., van Belle, G. T., and Zavala, R. T., "The Navy Precision Optical Interferometer (NPOI): an update," *J. Astron. Instr.* **2**, 1340002 (2013).
- [4] Hindsley, R. B., Armstrong, J. T., Schmitt, H. R., Andrews, J. R., Restaino, S. R., Wilcox, C. C., Vrba, F. J., Benson, J. A., DiVittorio, M. E., Hutter, D. J., Shankland, P. D., and Gregory, S. A., "Navy Prototype Optical Interferometer observations of geosynchronous satellites," *Appl. Optics* **50**, 2692–2698 (2011).



## SPECTROGRAPH 2

Figure 3. Fringe power as a function of fringe scanning frequency  $k$  fringes per modulation period in DirecTV-7S Spectrometer 2 data from March 6. Each frame corresponds to a spectral channel, with wavelengths from 845 nm (ch1) to 604 nm (ch12). This spectrometer observed only the W4-AC baseline, which had a fringe scanning frequency  $k = 1$ . The black line shows the power spectrum obtained with the coherent (on-fringe) scan. The red line is the power spectrum bias<sup>12</sup> obtained using an incoherent (off-fringe) scan, scaled based on the flux ratios of the coherent and incoherent scans. The green line is the bias-corrected power spectrum.



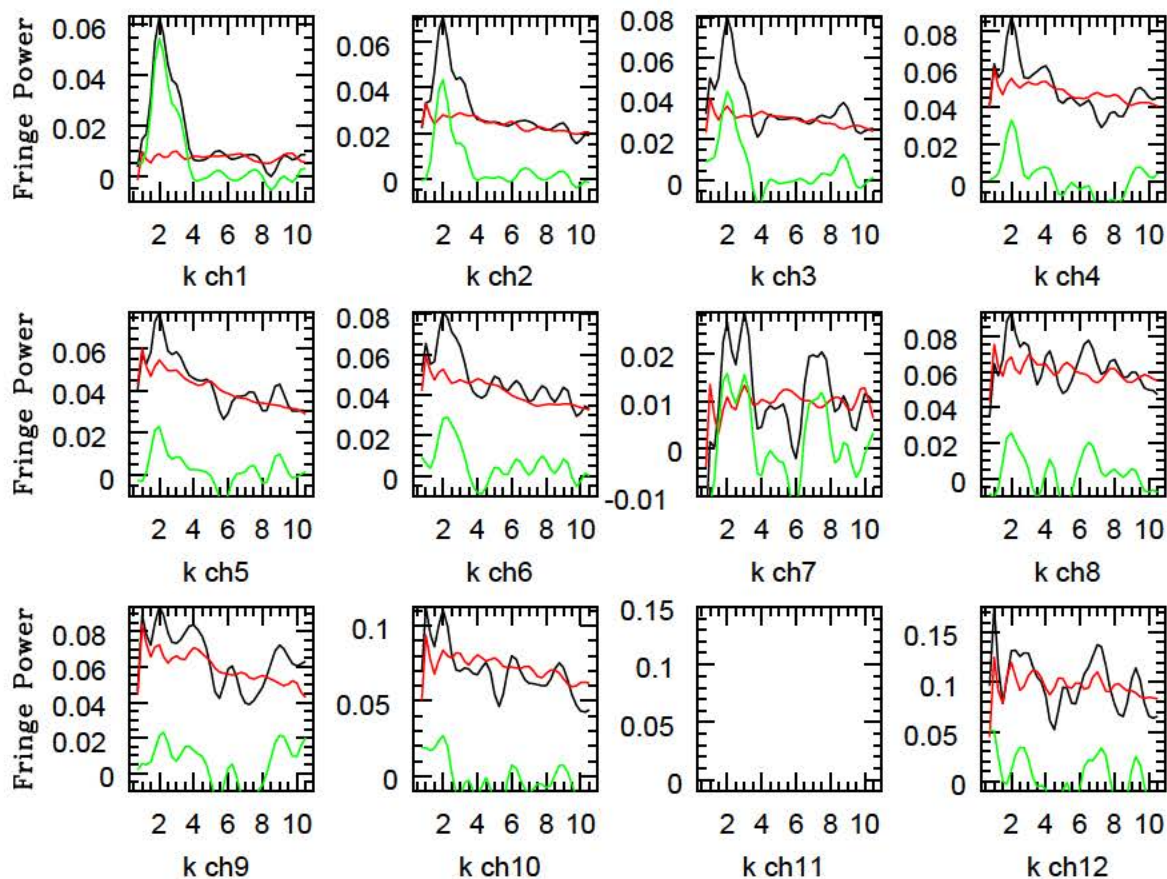


Figure 4. Fringe power as a function of fringe scanning frequency  $k$  fringes per modulation period in Spectrometer 1 data from March 6. This spectrometer observed all three baselines, W4-E3, W4-AC and AC-E3, with fringe frequencies  $k = 1, 2$  and  $3$ , respectively. As in 3, the black, red, and green lines show coherent (on-fringe), bias (off-fringe), and bias-corrected power spectra, respectively. Channel 11 is a dead channel.



- [5] Roddier, F., "Passive versus active methods in optical interferometry," in [*High-Resolution by Interferometry*], Merkle, F., ed., *ESO Conference and Workshop* **29**, 565–574 (1988).
- [6] Jennison, R. C., "A phase sensitive interferometer technique for the measurement of the fourier transforms of spatial brightness distributions of small angular extent," *Mon. Not. R. Astron. Soc.* **118**, 276–284 (1958).
- [7] Ducati, J. R., "VizieR online data catalog: Catalogue of stellar photometry in johnson's 11-color system," *VizieR Online Data Catalog* **2237**, 0 (2002).
- [8] Ramrez, I., Michel, R., Sefako, R., Tucci Maia, M., Schuster, W. J., van Wyk, F., Meléndez, J., Casagrande, L., and Castilho, B. V., "The ubv(ri)<sub>c</sub> colors of the sun," *Astrophys. J.* **752**, 5–13 (2012).
- [9] Fliegel, H. F., Warner, L. F., and Vrba, F. J., "Photometry of global positioning system block II and IIA satellites on orbit," *J. Spacecraft and Rockets* **38**, 609–616 (2001).
- [10] Sanchez, D. J., Gregory, S. A., Werling, D. K., Payne, T. E., Kann, L., Finkner, L. G., Payne, D. M., and Davis, C. K., "Photometric measurements of deep space satellites," in [*Imaging Technology and Telescopes*], Bilbro, J. W., Breckinridge, J. B., Carreras, R. A., Czyzak, S. R., Eckart, M. J., Fiete, R. D., and Idell, P. S., eds., *Proc. SPIE* **4091**, 164–182 (2000).
- [11] Vrba, F. J., Fliegel, H. F., and Warner, L. F., "Optical brightness measurements of GPS Block II, IIA, and IIR satellites on orbit," in [*Proceedings of the Advanced Maui Optical and Space Surveillance Technologies Conference*], (2003).
- [12] Hummel, C. A., Benson, J. A., Hutter, D. J., Johnston, K. J., Mozurkewich, D., Armstrong, J. T., Hindsley, R. B., Gilbreath, G. C., Rickard, L. J., and White, N. M., "First observations with a co-phased six-station optical long-baseline array: Application to the triple star  $\eta$  Virginis," *Astron. J.* **125**, 2630–2644 (2003).